Revista Cubana de Meteorología

Revista Cubana de Meteorología, Vol. 27, No. 2, April-June 2021, ISSN: 2664-0880

Artículo Original

Fog/haze events forecast validation using the mesoscale model WRF

Validación del pronóstico de eventos de niebla/neblina a través del modelo mesoescalar WRF

https://eqrcode.co/a/ChnFeO

Lic. Pedro Manuel González Jardines[1*], Dra. Maibys Sierra Lorenzo[2], Msc. Carlos Manuel González Ramírez[3], Lic. Israel Borrajero Montejo[4]

[1]Jose Martí ,International Airport, Boyeros Ave, Havana, Cuba.
[2]Center for Atmospheric Physics, Institute of Meteorology, Casablanca, Havana, Cuba.
[3]Provincial Meteorological Center La Habana-Artemisa-Mayabeque. Institute of Meteorology, Casablanca, Havana, Cuba.
[4]Center for Atmospheric Physics, Institute of Meteorology, Casablanca, Havana, Cuba.

ABSTRACT: The main objective of this research is the validation of numerical tools used for fog/haze events forecasting over the national territory. It is an extension of the SisPI project (Short range Forecasting System, with Spanish acronym) working operationally at the Institute of Meteorology (INSMET, with Spanish acronym). Version 3.8.1 of the mesoscale model WRF-ARW is used, initialized at 00:00 and 06:00 UTC to evaluate the impact of initialization on forecasts. As study area, it is chosen the region comprising the provinces of Havana, Artemisa and Mayabeque, which has ten conventional weather stations, divided into North coast, inner zone and South coast, for a more detailed assessment. Main absolute errors and linear correlations of the variables involved in the genesis and evolution of these phenomena were calculated allowing to determine a tendency to overestimate the values predicted on the study area. Contingency tables for binary events are also used for forecast evaluation, which show that the use of a cumulative distribution function allows a high degree of detection of these phenomena.

Palabras clave: nieblas, neblinas, visibilidad, probabilidad, sondeos numéricos, WRF.

RESUMEN: El objetivo esencial de la presente investigación es la validación de herramientas numéricas orientadas al pronóstico de eventos de niebla/neblina sobre el territorio nacional. Es una extensión del proyecto SisPI (Sistema de Pronóstico Inmediato) que trabaja operacionalmente en el Instituto de Meteorología (INSMET). Se emplea el modelo mesoescalar WRF-ARW en su versión 3.8.1 inicializado en los horarios de las 00:00 y 06:00 UTC para evaluar el impacto del horario de inicialización sobre el pronóstico. Se escoge como área de estudio la región que comprende las provincias de La Habana, Artemisa y Mayabeque, que cuenta con 10 estaciones meteorológicas convencionales, divididas en costa norte, interior y costa sur para obtener una evaluación más detallada. Se calcularon errores medios y correlaciones lineales de las variables implicadas en la génesis y evolución de estos fenómenos, lo cual permitió determinar una tendencia a la sobreestimación de los valores pronosticados en el área de estudio. Se emplearon además tablas de contingencia para eventos binarios con el propósito de evaluar el pronóstico, lo cual arrojó que el empleo de una función de distribución acumulativa permite un alto grado de detección de estos fenómenos.

Keywords: fog, haze, visibility, probability, numerical sounding, WRF.

INTRODUCTION

The fog/haze events forecast is a constant concern of the national weather service. In regard to these phenomena it is essential to consider the dynamic and synoptic characteristics that determine the boundary layer, as well as its variation with respect to the time scale, to adequately predict their extent, intensity and duration.

Some statistical tools have been developed with the purpose of predicting fog/haze events and are based primarily on the climatology. Using a conditional climatology has greater value than simple climatology but its main limitation is that it does not adequately consider the dynamic processes and gives more weight to the available data.

In the decade of the nineties, some numerical forecasting models were develop for fog forecast. (Golding , 1993) used a mesoscale general purpose numerical weather forecast model to simulate the development of fog in Perth, Australia. This result shows that terrain local inequalities and the development of local nocturnal winds can often determine the location and the opportunity of fog/haze to appear.

*Autor para Correspondencia: *Pedro Manuel González Jardines*. E-mail: pedro.met90@gmail.com
Received: 16/01/2021
Accepted: 01/05/2021

(Bergot & Guedalia. 1994) detailed an improved prognosis of radiation fog using a nocturnal one-dimensional boundary layer scheme, fed with an operational three-dimensional limited area mesoscale model. This paper shows the correlation between the observed data and predictions made by the proposed model. The influence of different physical processes including the dew deposition is also determined

Currently, the rapid advance of the numerical models, particularly the mesoscale model WRF (Weather Research and Forecasting) with a dynamical core ARW (Advanced Research WRF) allows introducing micro-physics, dynamic and planetary boundary layer characteristics that manage to reproduce, in real time and with sufficient accuracy, the environments in which processes of fog/haze develop. In this regard is included the doctoral thesis of (Ryerson, 2012) which proposes the use of an ensemble method of fog/haze forecast for ranges up to 20 hours.

Most national studies make reference to nocturnal irradiation processes in the formation of the aforementioned phenomena (Alfonso & Florido, 1980). However, it cannot be ruled out that due to horizontal transport of warm and humid air in the Southeast region synoptic flux that prevails when these phenomena occur, two kinds of fog can take place: advection and radiation. Other studies describe synoptic conditions associated with these events, highlighting those of days ahead of a cold front approximation and the presence of weak pressure gradients under a strong anti-cyclonic influence. (Guzmán, 2013).

This investigation evaluates a group of numerical tools oriented to fog/haze events forecasting using the mesoscale model WRF-ARW. To do this, forecasts obtained are evaluated for varying sea level pressure, wind force and direction, relative humidity, ambient temperature and dew point temperature, processes that are all involved in the genesis and development of fog/haze events. Subsequently, by using numerical soundings, visibility fields and cumulative distribution functions based on Weibull parameters, forecast maps are created by comparing days where the phenomenon occurred with those in which it is not present under similar synoptic conditions.

Fig. 1. Study area

MATERIALS AND METHODS

Study area

In the region including the provinces of Artemisa, Havana and Mayabeque, the occurrence of fog and haze has a low frequency; these are mostly of seasonal and local character, related largely to physical and geographic characteristics. They are associated with the second quadrant flux imposed by the periphery of the subtropical anticyclone, situation that precedes the arrival of a frontal system or the influence of weak pressure gradients (Guzmán, 2013).

Additionally it should be noted that this region is of extraordinary social and economic importance as it has a high agricultural and industrial development. Just to mention some examples, there is the Mariel Exclusive Economic Zone with a growing importance of port activities and transport of goods. In addition, livestock and agriculture, have an increasing activity, there are large areas dedicated to these purposes mainly in the provinces of Artemisa and Mayabeque, with high demand crops such as garlic, onions and potatoes.

Southeast of the capital, José Martí International Airport is one of the largest airport facilities in the Country that given its locations, is affected by these phenomena mainly during the dry season (that extends from November to April), sometimes causing delays in the normal development of their duties. In the Baracoa zone (Artemisa province) lies another airport where the fog/haze forecast is also necessary. It's also relevant to mention that it is a densely populated region as the capital only has more than two million inhabitants.

Study cases

Based on the information from present time data codes reported at stations and comprising hours between 00:00 and 12:00 UTC six study cases were selected, corresponding to the dry season of 2017. The six selected cases were divided into three couples of continuous days, considering that there were significant differences (in both spatial-temporal extension and intensity) in fog/haze outbreaks between one day and the next under similar synoptic conditions. This has the purpose of evaluating the sensitivity of the model to these changes.

The first pair of days comprises January 26th and 27th. The 26th was characterized by weak influence of the subtropical ridge, imposing a southeast wind regime over the study area, while a cold front, weakened at its southern portion, was passing over the center-eastern region of the Gulf of Mexico. The next day shows the above conditions with a slightly strengthened anticyclone center and the weakened cold front moving over the peninsula of Florida, which advanced

toward the north of the study area during the remainder of the 27th.

The second pair of days includes February 8th and 9th, which were characterized by a marked influence of high pressures with an extended oceanic ridge over the eastern portion of the Gulf of Mexico. A greatly weakened cold front moved by the southeastern United States, which did not affect the western of the country. The pressure gradients weakened considerably towards the early 9th, resulting in a small secondary center northwest of the island during the morning that quickly disappeared with the advance of a migratory anticyclone accompanied by the new air mass.

Finally, April 5th and 6th were included. The 5th was characterized by the influence of an oceanic anticyclone that extended its dorsal into the Gulf of Mexico, imposing a second quadrant flux, at the same time a well-structured cold front advanced toward the western portion the Gulf of Mexico. On the early morning of day 6th, the front reached the East of the gulf and started to affect the study area during the afternoon.

WRF-ARW model experiments design

The experiments were executed using version 3.8.1 of WRF-ARW with the operational configuration used by SisPI (Sierra *et al.,* 2014) which has two way nested outer domains, with horizontal resolutions of 27 and 9 kilometers (km) respectively and a single one way nested inner domain of 3 km enabled through the use of the ndown tool.

The temporal resolution of the first two domains is three hours while the 3 km domain provides forecasts every hour. For the initial and boundary conditions the GFS (Global Forecast System) data forecast was used with spatial resolution of 0.5 degrees and temporal resolution of three hours.

An element to take into account, in addition to the purely meteorological considerations is the model spin-up. A model spin-up effect can matter on some phenomena forecasts and determinate its detection or not.

Following this reasoning, an analysis was made about how close to the initialization the phenomenon should be. Given that the most frequent hours of fog/haze occurrence is 12:00 UTC (Álvarez *et al*., 2011) it was decided to evaluate the predictions made by the WRF initialized at 00:00 and 06:00 UTC.

The parameterizations set used by SisPI for the 3 km domain includes the Morrison double moment scheme for microphysics, which is a second order representation of the processes of ice, snow, rain and graupel, it does not apply cumulus parameterization, as at high resolutions the convective precipitation can be solved with the microphysics scheme, it also uses the Mellor-Yamada Nakanishi and Niino (MYNN) 2.5 level TKE boundary layer scheme, which predicts the terms of kinetic energy at subgrid level.

The ARWpost package version 3.1 was used for post-processing, this post-processing package is avaliable at following direction (https://www2.mmm.ucar.edu/wrf/users/download), along with GrADS (Grid Analysis Display System) scripts. A script made in shell language automated the entire process. In the simulations, a number of diagnostic variables were calculated, that the Air Force Weather Agency (AFWA) used in its operational model MEPS (Mesoscale Ensemble Prediction Suite) (Creighton *et al.*, 2014).

Most of these diagnoses are only calculated for output time steps, as they are just snapshots of the modeling environment. However, one of the benefits of running diagnostics in-line is the ability to collect information on the rapidly evolving fields between output time's steps, although it involves an additional computational cost.

Values related with a visibility reduction due to hydrometeors, dust and fog or haze are used as a Weibull β value and a prognostic Weibull alpha value is used if lowest visibility is associated to haze or fog. The alpha term is dimensionless and describes the shape of the Weibull curve, it behaves more like a Gaussian curve when absolute humidity is high and more like an exponential when the absolute humidity is low. The practical implication of this is to ensure the highest probability of reduced visibility in the mid-range of 4.83 to 8.05 km (3-5 miles) (Creighton *et al*., 2014).

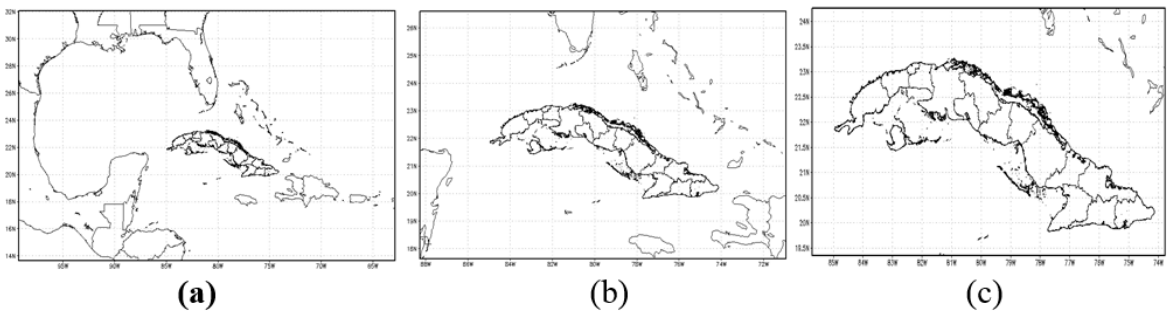

Fig. 2. Operative SisPI domains. (a) 27 km, (b) 9 km, (c) 3 km.

The alpha term is calculated as follows:

$$a_{fog} = 0.1 + \frac{Pwat}{25} + \frac{Wind}{3} + \frac{rh}{10} + \frac{1}{mix} \quad (1)$$

where *Pwat* is the precipitable water, *Wind* is the 100 meters height wind, *rh* is the relative humidity at 2 meters and *mix* the mixing ratio at 2 meters. The value of this parameter is 3.6 and its decrease implies that the BIAS shifts toward a fog/haze event.

The empirical algorithm used by (Creighton *et al*., 2014), is based on relative humidity and the visibility values, in meters, is obtained by equation (2):

$$Vis_{meters} = \left(\mathrm{Vis}_{\mathrm{Hydro}}, \mathrm{Vis}_{\mathrm{Dust}}, \mathrm{Vis}_{\mathrm{fog}}\right) \quad (2)$$

where the visibility due to dust obscuration is calculated only for WRF-CHEM simulations and the visibility due to hydrometeors and fog/haze areas obtained using:

$$Vis_{hydro} = \frac{3.912}{1.1 * (Rain + Graupel)^{0.75} + 10.36 * (Snow)^{0.78}} \quad (2.1)$$

where rain, graupel and snow are mass concentrations in g/m^3.

$$Vis_{fog} = 1500 * (105 - rh) * \left(\frac{5}{mix}\right) \quad (2.2)$$

where rh is 2 meter relative humidity and mix is 2 meters mixing ratio.

By combining the elements just described, it is possible to determinate, the probability of occurrence of a fog/haze event from the definition provided by the World Meteorological Organization (WMO), using a cumulative distribution function (CDF):

$$CDF(X) = \left(1 - e^{\frac{-(X - Xo)}{\beta} * \alpha}\right) * 100 \quad (3)$$

This function determines the probability of obtaining a value less than or equal to X. Beta in this case, determines the shape of the distribution curve, is assumed from the visibility value calculated in equation (2) and alpha is explicitly obtained for this phenomenon, as shown in equation (1). (Creighton *et al*., 2014).

In order to obtain a more detailed analysis of the results the study area was divided into three regions, meeting the criteria of subdivisions used at INSMET (Cuban Meteorological Institute, with acronym in Spanish) for the assessment of forecasts.

These sub-regions were designed taking into account the meteorological stations that had a similar statistical behavior. These sub-regions are divided into North coast, comprising the stations Bahía Honda (318), Bauta (376) and Casablanca (325), South coast, including Güira de Melena (320), Batabanó (322) and Melena del Sur (375) stations and the inner subregion which encompasses stations Santiago de Las Vegas (373), Tapaste (374), Bainoa (340) and Güines (323).

For a statistical evaluation, the mean absolute error considering the observation (O) minus the prediction (P), (O-P) for the all analysis cases and also the Pearson correlation coefficient described in equation (4) were calculated.

$$r = \frac{n * \sum (x_i * y_i) - \sum x_i * \sum y_i}{\sqrt{\left(n * \sum x_i^2 - 2\right) * \left(n * \sum y_i^2 - 2\right)}} \quad (4)$$

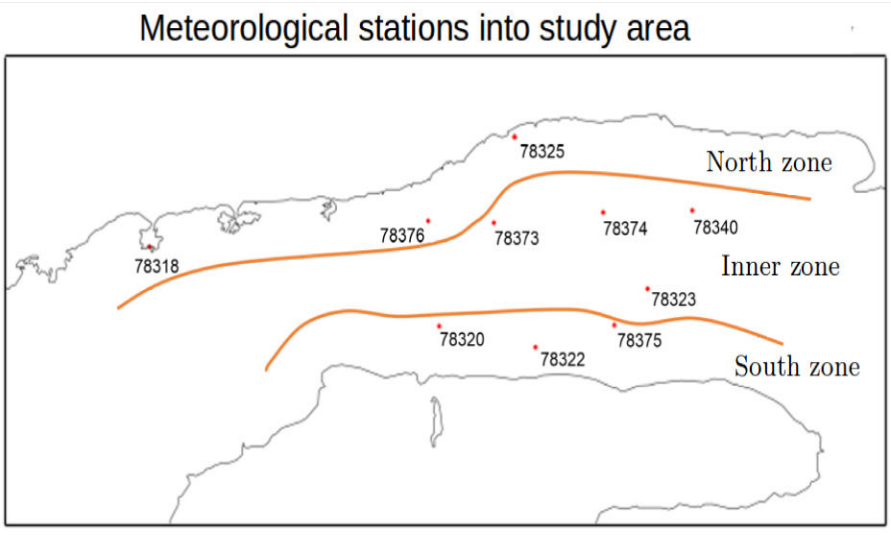

Fig. 3. Sub-regions inside the study area

Table I. Contingency table for binary events.

Event forecast	Event observed	
	Yes	**No**
Yes	Hit	False alarm
No	Miss	Correct rejection

Table II. Thresholds of variables involved in the occurrence of fog/haze events (Hernández *et al.*, 2017)

(a)				
Month	**Wind speed (km/h)**	**Temperature (ºC)**	**Dew Point (ºC)**	**Relative humidity (%)**
January	0.9 - 2.0	14.8 - 20.0	14.3 - 20.7	96.2 - 99.0
February	0.2 - 8.6	15.6 - 21.0	15.1 - 20.0	96.2 - 98.0
April	0.0 - 5.0	18.6 - 22.7	17.7 - 21.7	94.1 - 98.5
(b)				
Month	**Wind speed (km/h)**	**Temperature (ºC)**	**Dew Point (ºC)**	**Relative humidity (%)**
January	0.0 - 4.6	15.0 - 20.0	14.0 - 20.0	92.0 - 96.6
February	1.0 - 4.7	15.0 - 20.4	14.0 - 19.0	91.0 - 95.8
April	0.0 - 6.0	19.0 - 22.8	18.0 - 21.6	89.8 - 94.9

Table III. Main absolute error for all study cases, (a) initialized at 00:00 UTC, (b) initialized at 06:00 UTC.

(a)							
Sub-regions	**T (ºC)**	**Td (ºC)**	**dd (º)**	**ff(km/h)**	**P (hPa)**	**RH (%)**	**Vis (km)**
North coast	-0.82	0.18	-46.49	-3.91	**-0.51**	-2.07	**-16.03**
Inner zone	**-2.10**	**-1.03**	**-70.03**	**-6.10**	-0.19	**-4.38**	**-16.62**
South coast	-1.09	-0.44	-30.90	-4.42	-0.05	-3.70	-12.09
(b)							
Sub-regions	**T (ºC)**	**Td (ºC)**	**dd (º)**	**ff(km/h)**	**P (hPa)**	**RH (%)**	**Vis (km)**
North coast	-1.76	-0.07	-22.98	-4.48	**-0.57**	0.61	-19.93
Inner zone	**-2.55**	**-0.64**	**-48.62**	**-7.25**	-0.19	0.64	-22.08
South coast	-1.31	-0.29	-19.14	-5.24	-0.14	**-1.52**	**-15.18**

The calculations were made through a program developed in C / C ++ platform and some graphics support with code developed in Octave; in both cases it was all included in the automation post-processing program.

Finally, a verification of numerical forecasts considering fog/haze occurrences as binary events is included. Such verification is made by using a contingency table considering alpha, visibility and CDF variables, which can explicitly predict the genesis/evolution/ dissipation of the event.

Based on the results obtained for the two initialization times in all study cases, hit rate (H) was obtained which indicates the proportion of occurrences that were correctly identified by the model. It is also included the probability of false detection (F), which indicates the proportion of occurrences that were incorrectly predicted and critical detection index (CSI).

$$H = \frac{a}{a+c} \quad F = \frac{b}{b+d} \quad CSI = \frac{a}{a+b+c} \quad 5)$$

DISCUSSION OF RESULTS

Relationship between real data and simulations with WRF

(Hernández *et al.*, 2017) defined thresholds for a number of variables involved in the genesis and development fog/haze processes in the study area. These thresholds were obtained for each month, from a sample that included 6372 haze cases and 904 fog cases; they are shown in table II.

The analysis done by calculating the mean absolute errors shows a tendency by the model to overestimate the values of all variables. The biggest errors are in the wind direction.

A determining factor in this regard is the fact that observers report zero for direction when there is calm, which significantly increase errors. Finally it should be mentioned that wind direction calculated by the model has a much greater variability than those measured by conventional station, although the estimation, from a qualitative point of view, is suitable.

An important issue related with fog/haze predictions is the fact that the model overestimates the wind force in the range between 1 and 10 km/h. This may result significant in some cases, because during the nocturnal irradiation processes, low wind speeds reduce turbulent mixing processes, which favors an increase in the relative humidity over surface allowing saturation process. The increased turbulence mixing due to stronger winds considerably limits the appearance of the phenomena, apparently because it dries the air as moisture loss increases due to dew formation or more intrusion of dry air at higher levels.

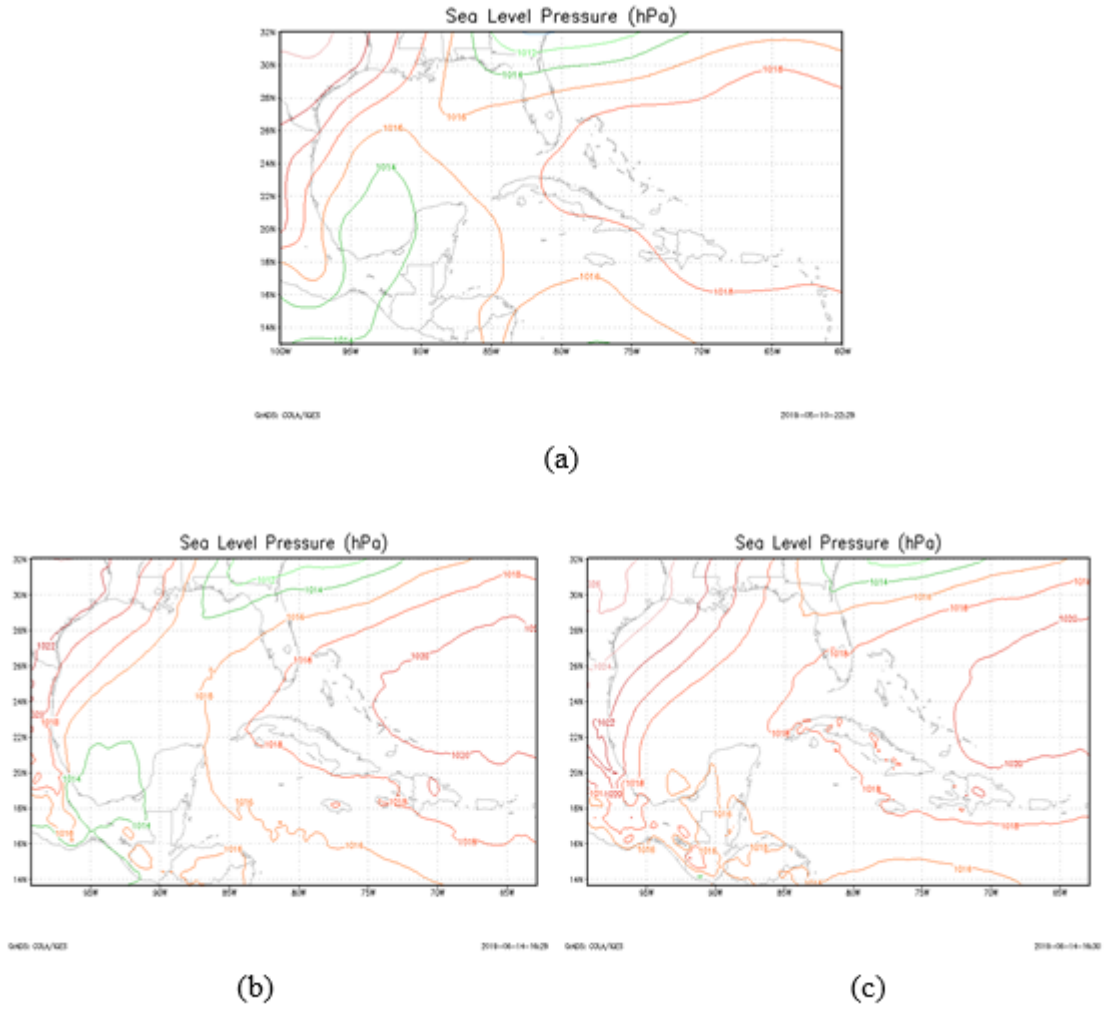

Fig. 4. Sea level pressure for January 26th, 12:00 UTC; (a) represent reanalysis fields; (b) forecast initialized at 00:00 UTC; (c) forecast initialized at 06:00 UTC.

WRF forecasts obtained for January 26th show the above-mentioned situation. In this case, the model overestimates the wind speed in the 8 to 10 km/h range, which was consistent with the worst fog/haze forecast over the study area. This bias is attributed to the fact that the model also overestimated the subtropical ridge strength and therefore the pressure gradients over the study area, which is corroborated by reanalysis data (Figure 4).

Another variable, which causes errors to grow significantly, is visibility. There is a factor that adds to the subjectivity inherent to these observations and acts indirectly on the error value. This is that all conventional stations estimate visibility from reference points with known distances to the station. This implies that all stations have a maximum visibility in the study area that does not exceed 15 km. This limitation imposes an upper limit to the value of visibility which the model does not have, since it obviously does not depend on any reference point. This causes the absolute daytime errors to grow significantly.

As general considerations it can be said that temperature, dew point pressure and relative humidity showed little errors that can be considered insignificant for the forecast ability, although for initializations made at 06:00 UTC these errors were slightly higher compared to those made at 00:00 UTC. Another interesting aspect is that the biggest errors are limited to the inner zone of study area. This can be caused by increased variability in the behavior of meteorological variables, which is limited in coastal regions because of the modulation effect of the sea.

Table 4 shows the behavior of the mean absolute error for the variables involved in the analysis at the times that, according to the information of present time code reports, the station detected fog/haze, values reveal some interesting aspects.

First it's observed how it decreases, by more than 10 km, the value of visibility forecast error, which confirms what is explained above. For runs made with initialization at 00:00 UTC, the model predicts more trusty visibility values than when initialized at 06:00 UTC. In the example of Figure (5) the significant dif-

Table IV. Main absolute error at times of phenomena apparition for all study cases, (a) initialization at 00:00 UTC, (b) initialization at 06:00 UTC.

(a)							
Sub-regions	**T (ºC)**	**Td (ºC)**	**dd (º)**	**ff (km/h)**	**P (hPa)**	**RH (%)**	**Vis (km)**
North coast	-0.26	**0.70**	-55.93	-3.41	**-0.89**	-1.67	-6.55
Inner zone	**-0.43**	-0.02	**-90.07**	**-4.55**	-0.74	**-0.87**	**-6.61**
South coast	-0.27	0.11	-22.89	-3.46	-0.48	-1.38	-4.54
(b)							
Sub-regions	**T (ºC)**	**Td (ºC)**	**dd (º)**	**ff(km/h)**	**P (hPa)**	**RH (%)**	**Vis (km)**
North coast	-1.53	-0.61	-69.53	-4.73	**-0.91**	**3.05**	-8.44
Inner zone	**-1.86**	**-1.07**	**-131.52**	-5.04	-0.69	2.61	**-9.84**
South coast	-0.89	-0.40	-49.67	-5.05	-0.44	1.93	-6.38

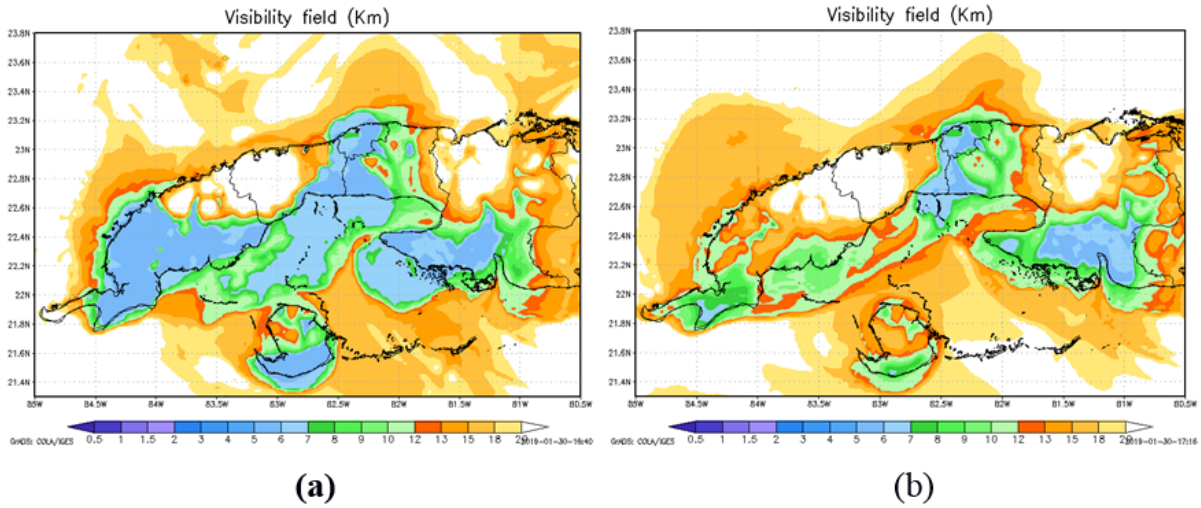

Fig. 5. Visibility fields forecast for February 9th at 12:00 UTC case, (a) initialized at 00:00 UTC, (b) initialized at 06:00 UTC.

Table V. Linear correlation, (a) initialized at 00:00 UTC, (b) initialized at 06:00 UTC.

(a)							
Sub-regions	**T**	**Td**	**dd**	**ff**	**P**	**RH**	**Vis**
North coast	0.70	0.34	0.78	**0.79**	0.49	0.38	**0.62**
Inner zone	0.78	0.37	0.80	0.64	**0.58**	0.14	0.59
South coast	**0.80**	0.36	**0.82**	**0.79**	0.51	0.29	0.52
(b)							
Sub-regions	**T**	**Td**	**dd**	**ff**	**P**	**RH**	**Vis**
North coast	0.69	0.35	0.71	**0.78**	0.54	0.36	0.63
Inner zone	**0.75**	0.38	**0.74**	0.74	**0.58**	0.06	**0.70**
South coast	0.57	0.45	0.70	0.47	0.34	0.22	0.47

ferences between both initializations for the forecast given at 12:00 UTC of February 9th can be appreciated, this pattern is reproduced in all cases studied.

The main cause of this difference is the fact that WRF was unable to detect favorable environment for fog formation during the first 6 hours of forecast, on the other hand, a 24 hours forecast shows no significant differences regardless of the initialization time.

All other variables showed no significant differences in the behavior of the main absolute error with regard to the tables where their general behavior is described. In fact, it is possible to appreciate that visibility reduction forecasts propagate the phenomenon from South to North, just as it really happens. This suggests that together with the irradiation process, the model identified an advective process, in this case, moisture, due to the persistence of weak flux from the Southeast - South that contributed to the expansion of the surface moist layer creating favorable environments for fog/haze genesis. The complementary linear correlation analysis yielded the following results.

In general, ambient temperature, the wind direction and speed, showed very good linear correlation, although in the case of initializations at 06:00 UTC va-

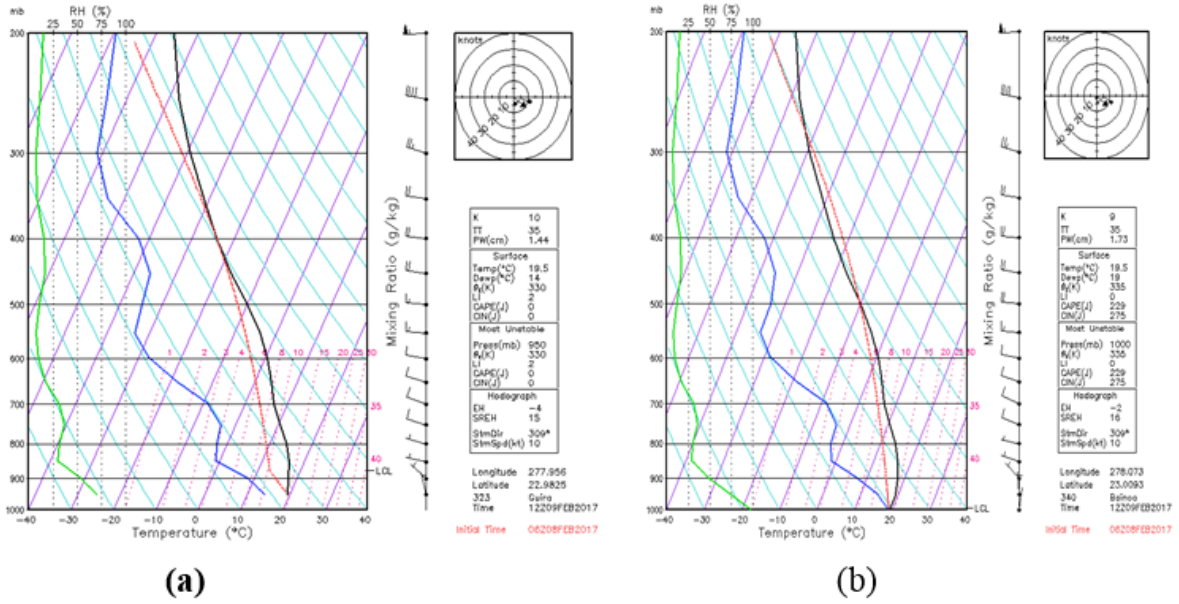

Fig. 6. Numerical soundings forecast on February 9th at 12:00 UTC initialized at 06:00 UTC February 8, (a) 323: station with haze, (b) 340: station with fog.

lues tend to be weaker; this can be attributed to greater variability in the behavior of variables predicted by the model in the initial forecast steps.

The visibility variable shows good linear correlation values located at close 0.6 value, with less variation towards north coast.

This can be in correspondence to the advection process occurring from the southern portion of the study area, which makes it a zone of exchange between air masses with different mesoscale features, the main difference lies in the content of humidity. Due to this exchange, the dynamics of the processes that occur here are not only somewhat different from the rest of the area, but it also changes quickly.

Relying on these results it is possible to use a linear regression equation to try to adjust the visibility value predicted by the model.

Dew point temperature, pressure at sea level and relative humidity variables exhibit weak linear correlations, however it is important to realize that they show the lower absolute errors, this is not a contradiction. The linear correlation coefficient is a summary measure that does not implies causality and in order to establish a cause-effect relationship there must be more elements. In this case, the value of the coefficient informs just that forecasts cannot be adjusted by employing a linear equation.

Numerical Soundings

From an aerological point of view, irradiation fog/haze formation is characterized by the presence of a thermal inversion in the lower layers of the atmosphere, due to heat released to higher layers. Essentially, it means that the heat accumulated during the day is released from surface toward the upper layers, which causes a sufficient surface cooling to allow moisture increase and water vapor condensation, resulting in the appearance of the phenomena.

Another common cause is the formation of subsidence fogs, these are cases, where under anticyclonic prevalence product of downward movements, the lower layer of the atmosphere is compressed and warmed slightly resulting in subsidence inversion.

In all cases analyzed the model was able to detect the conditions that must be present in the vertical structure for the development of these phenomena, such as the presence of a saturated layer next to surface, the high relative humidity over surface and presence of dry air at high altitude, the presence and location of an inversion just above the saturated layer, where a temperature increase and dew point reduction is noted, weak winds on the boundary layer and finally a moderate vertical shear near the inversion that traps the lower layers.

The numerical soundings made for all study cases suggest that the greatest inversion intensity is directly associated with the occurrence of an event of fog, while the distinction between a haze event and the no occurrence of fog/haze processes is much weaker, this result is consistent with the views expressed by (Guzmán, 2013).

Another important agreement with this study, where real sounding were used, is the fact that the first temperature inversions associated with fogs are the most powerful; which means that they have larger vertical temperature gradients and occur at lower altitudes. In cases of study reviewed in the present research, inversion with gradients equal or greater than 1 Celsius degree every 50 hPa (hectopascals) matched fog pre-

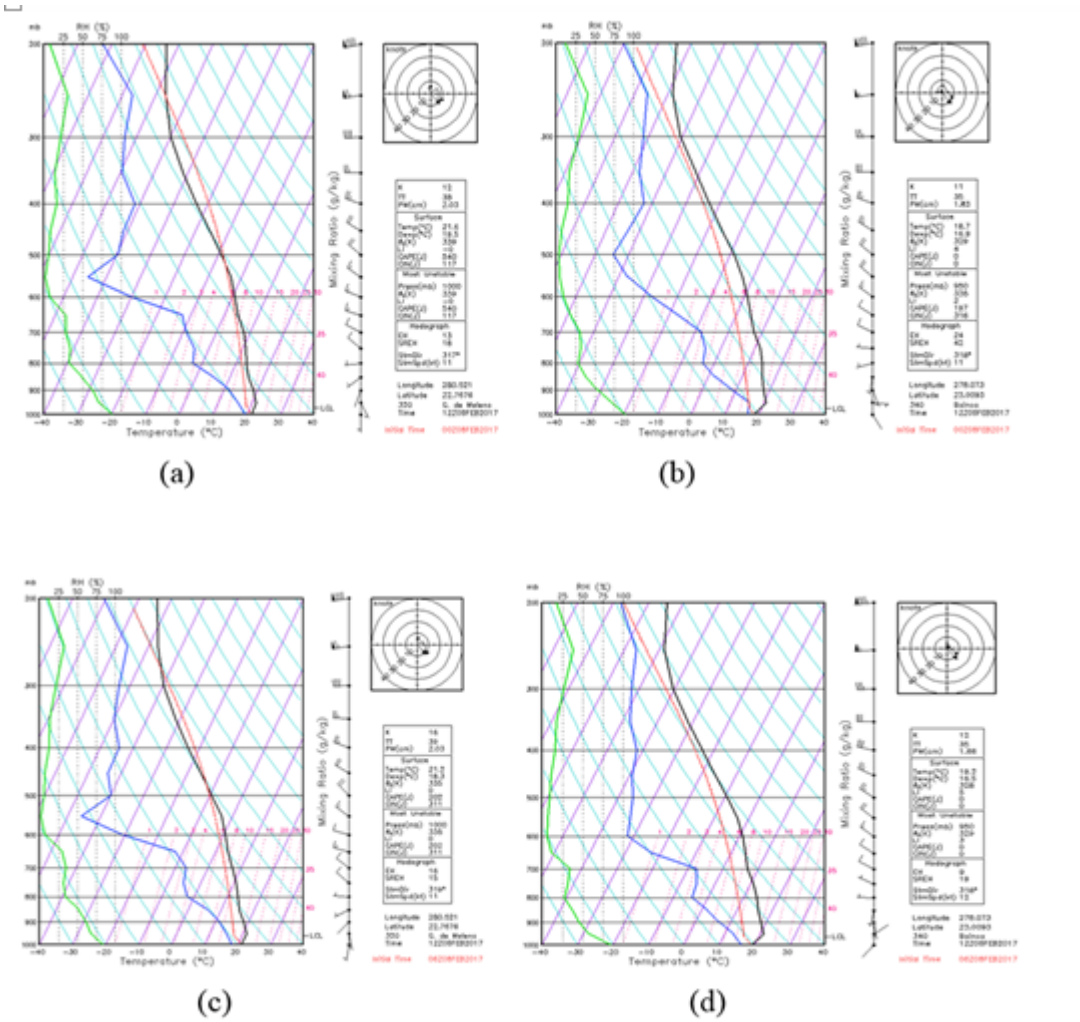

Fig. 7. Forecast for meteorological stations 320 and 340 on February 8th; (a-b) initialized at 00:00 UTC; (c-d) initialized at 06:00 UTC; saturated layer intensity is underestimated for cases initialized at 06:00 UTC.

sence and they are located in the layer between 1000 and 900 hPa, on the other hand, in haze cases the gradient was much smoother or almost nonexistent with a very weak inversion located next to the intermediate layers between 850 and 600 hPa. As far as the the model is concerned, the temperature gradient along the inversion is more important that the depth of it.

In conditions where the model detects surface relative humidity values of about 90%, with weak inversions, it is considered as a hostile environment for the development of fog/haze. This result is related to the thresholds established by *(* Hernández *et al.,* 2017 *)* for the study area and the results of (Guzmán, 2013), which determined that the most intense vertical gradients are associated to the development of fog.

These results are consistent with the fact that as the intensity of the irradiation process increases; the gradual cooling of superficial layers increases the static stability near surface and thus the inversion intensity, reducing friction on surface and leading to a decoupling between moving air in the region above the inversion layer. Under these conditions it is important to consider the thickness of the wet layer located under the inversion, since the process of fog/haze can intensify or dissipate depending on the nature of the adjacent air.

Forecasts based on the CDF

The use of the alpha Weibull parameter, as well as the results of the CDF, offers an additional option for spatial forecasting of fog/haze events.

An example of the resulting forecast parameter is given in Figure (8). It notably reflects the dynamic character associated with the formation of irradiation fog as it considers the thickness of the wet layer next to the surface, as well as the turbulent mixing process involved in the development or dissipation of the event, both elements can interact shaping the characteristics of the fog/haze event.

In the case corresponding to January 26th, where there was an overestimation of pressure gradients, the turbulence associated with relatively stronger winds, allowed the intrusion of drier air from higher levels

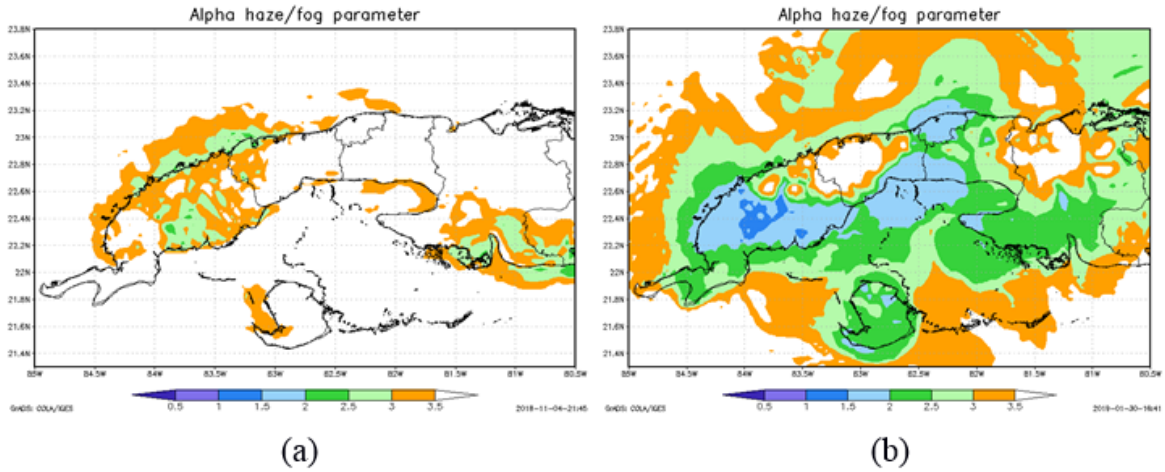

Fig. 8. Alpha parameter forecast at 12:00 UTC initialized at 00:00 UTC; (a) January 26th case; (b) February 9th, case.

combined with a limited cooling irradiation rate due to the synoptic flux, according to this logic WRF identified a hostile environment for the appearance of the phenomenon. As has been described above, the real conditions for this day were characterized by very weak pressure gradients and wind speeds ranging between 0 and 2 km/h in all meteorological stations. This case is an example of how complex it is for numerical models to predict favorable environments for the development of fog/haze events.

For the rest of the study cases, the model correctly predicted real conditions, which led to successful predictions.

The example of Figure (9) shows the characteristic behavior of the alpha parameter, showing that those values below 3.5 suggest potentially favorable environments for fog/haze development, which is consistent with forecasts obtained from numerical sounding. In this particular case, stations reported fog, but both, numerical soundings and the alpha parameter forecasted the phenomenon only for stations 340 and 320, and not for station 374.

Regarding Tapaste station (374), there are physical and geographical peculiarities that contribute to a greater difficulty for fog/haze forecast, this could be seen on all case studies. This is given in the first instance, because the station is at 120 meters (m) above sea level, being the highest of all that make up the study area. It also lies inside a depression, surrounded by regions exceeding 200 meters high and has abundant vegetation. Fogs in this area are further characterized by an elevated dew deposition rate which leads to suspicions of advective processes existence that maintain the necessary moisture supply at low levels to support the apparition of the phenomenon.

Although the topographical model information reflects with remarkable precision these topographic characteristics, it underestimates the heights around the station, toward the north coast and mainly the Melena-Madruga heights southward of the inner plateau.

Since the orographic component is significant to analyze the presence or not of fog/haze, this is a possible cause for WRF to fail detecting favorable environments for fog/haze genesis and evolution on that portion of the study area. Undoubtedly in this area local circulations take place, product of the orographic differences, which WRF dynamics fails to accurately represent.

Probability values calculated by the model successfully meet the visibility field variations, registered by the stations over the study area with maximum values when visibility is minimal or fog/haze events are detected as illustrated in Figure (11). The graphics show how predicted probability values react adequately to visibility reduction because of the existence of fog/haze phenomena. More specifically, values of probability greater than or equal to 75% suggest that the visibility can be reduced to the point of being associated with a fog/haze phenomenon.

It cannot be overlooked that the fog/haze manifestation is partial in many cases, which causes the observer to codify the phenomenon on the present time code but simultaneously to report a visibility greater than 5 km.

This clearly subjective consideration makes difficult the forecast homogenization made by the model, on the other hand, visibility values of less than 3 km were never registered. Seeking to establish a uniform approach, it was decided that the most appropriate criterion is that from the World Meteorological Organization (WMO) where the reduction of visibility to less than 1 km is associated with fog and between 1 and 5 km to haze.

The generation of these maps involves some practical considerations. In the first place the problem of initialization time comes to light again because the closeness of the initialization to the possible occurrence of the phenomena brings a decrease in the ability of the model to detect them, a characteristic that was appreciated in all study cases. This is an expected

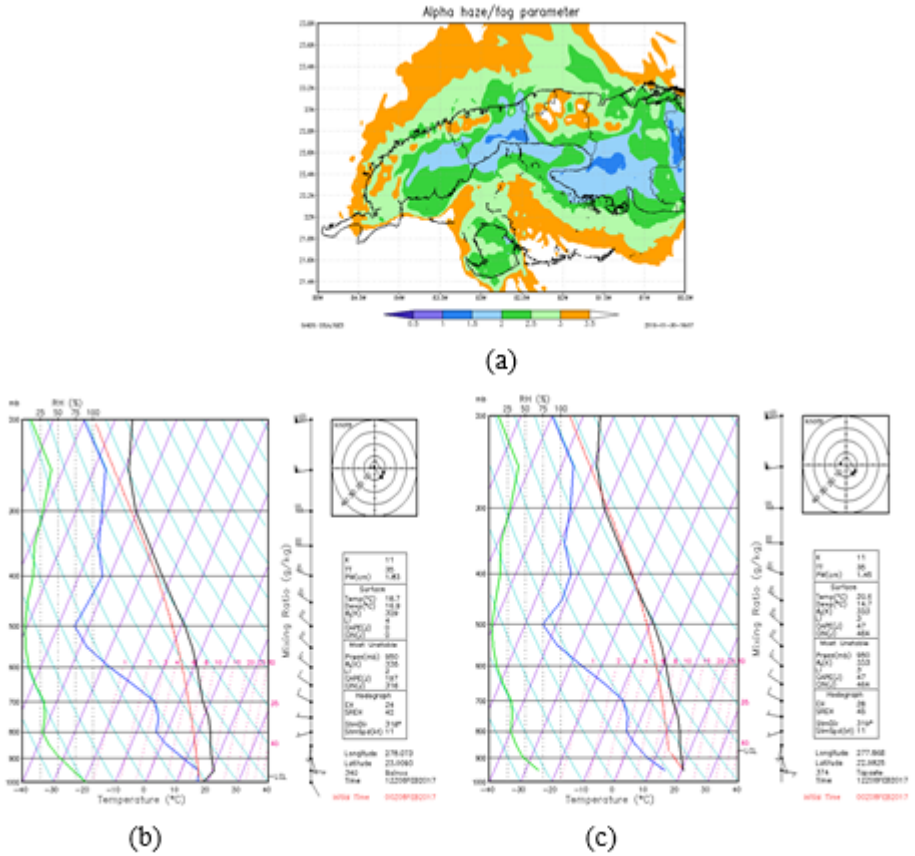

Fig. 9. Relation between numerical sounding and alpha parameter forecast made on February 8th, 12:00 UTC, initialized at 00:00 UTC; (a) alpha parameter; (b) weather station 340, (c) weather station 374.

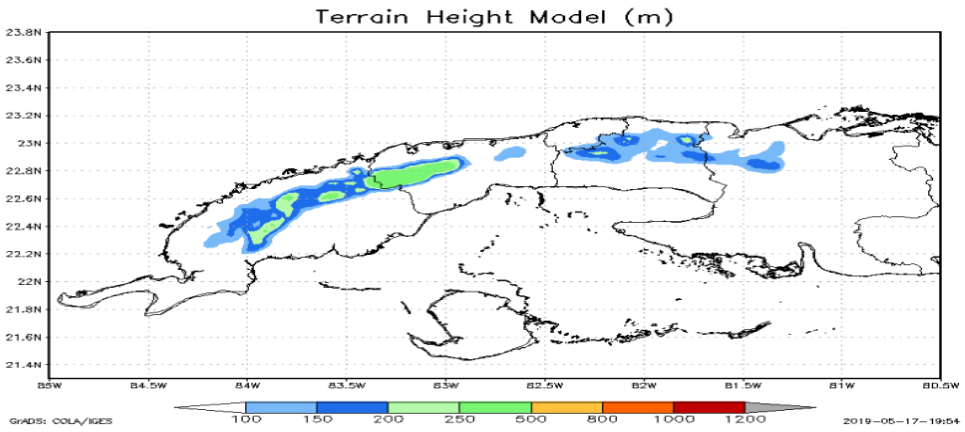

Fig. 10. Terrain height available in WRF.

result for this variable, because, as it was expressed in equation (3), the calculation is dependent on the alpha value and the visibility field, which makes it a resume variable where the dynamic character directly associated with the fog/haze formation over the study area is contained.

One issue that should not go unmentioned is the fact that the model has a trend to anticipate the formation of the phenomena and its dissipation start at around 12:00 or 13:00 UTC, with a maximum between 10:00 and 11:00 UTC. However, from the point of view of operational fog/haze forecasting this shift does not represent any obstacle.

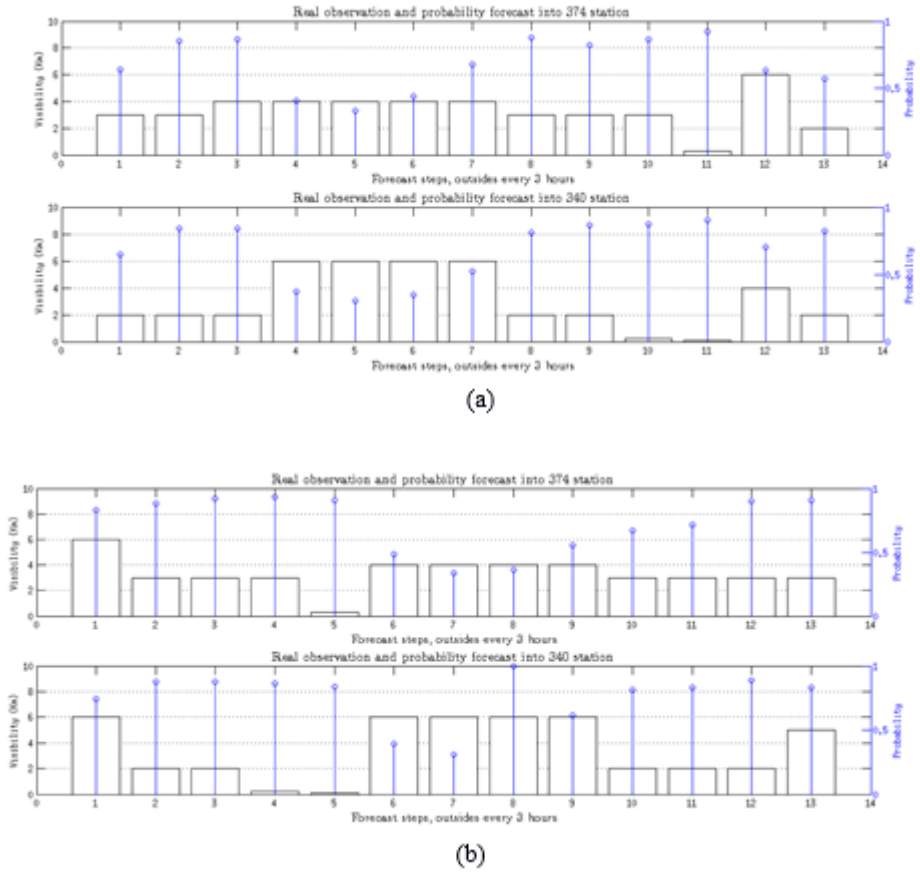

Fig. 11. Relationship between visibility observed and probability forecast for meteorological stations 340 and 374; (a) April 5th case, (b) April 6th case, both initialized at 00:00 UTC.

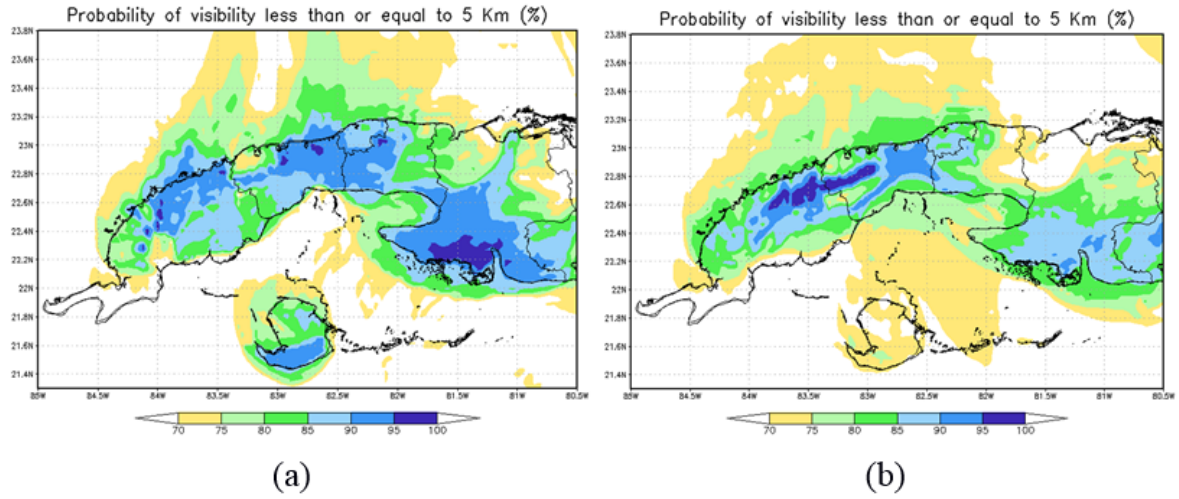

Fig. 12. Fog/haze probability forecast on April 6th, 11:00 UTC; (a) initialized at 00:00 UTC; (b) initialized at 06:00 UTC

There are three variables available, able of explicitly predicting favorable environments for fog/haze occurrence, however not all detected the phenomenon equally. To learn more in detail the detection ability of these variables, a forecast verification was made considering these phenomena as binary events, detection and non-detection, which yielded the following results.

The results reflected in the tables reveal that visibility fields have a poor performance in fog/haze detection, which is given by the fact that the variable is overestimated on just over 80% of the forecast outputs, the number of occurrences correctly predicted oscillate between 20 and 30% only. The alpha parameter improves significantly this relationship, despite an increase seen in false alarms, especially in the initia-

Table VII. WRF Forecast verification; (a) Initialized at 00:00 UTC; (b) Initialized at 06:00 UTC

(a)									
Cases initialized at 00:00 UTC									
	Visibility field			**Alpha parameter**			**Accumulative distribution function**		
	POD	**POFD**	**CSI**	**POD**	**POFD**	**CSI**	**POD**	**POFD**	**CSI**
North coast	0.31	0.01	0.30	0.64	0.20	0.44	0.79	0.28	0.50
South coast	0.45	0.03	0.42	0.69	0.44	0.36	0.90	0.48	0.46
Inner zone	0.23	0.009	0.23	0.68	0.41	0.41	0.76	0.31	0.55
(b)									
Cases initialized at 06:00 UTC									
	Visibility field			**Alpha parameter**			**Accumulative distribution function**		
	POD	**POFD**	**CSI**	**POD**	**POFD**	**CSI**	**POD**	**POFD**	**CSI**
North coast	0.23	0.01	0.22	0.70	0.22	0.46	0.67	0.22	0.43
South coast	0.24	0.03	0.23	0.64	0.30	0.37	0.83	0.34	0.46
Inner zone	0.08	0.02	0.08	0.61	0.27	0.44	0.60	0.37	0.47

Tab. VIII. WRF full forecast verification.

Full cases forecast verification.									
	Visibility field			**Alpha parameter**			**Accumulative distribution function**		
	POD	**POFD**	**CSI**	**POD**	**POFD**	**CSI**	**POD**	**POFD**	**CSI**
North coast	0.27	0.01	0.26	0.67	0.21	0.45	0.73	0.26	0.41
South coast	0.34	0.03	0.33	0.66	0.36	0.36	0.87	0.29	0.46
Inner zone	0.16	0.01	0.16	0.64	0.68	0.44	0.78	0.29	0.56

lizations made at 00:00 UTC, this is due primarily to the fact that it tends to anticipate the genesis and dissipation of the event.

The value given by the accumulated distribution function, offers the best results. In this sense, it is worth remembering that the visibility measurement largely depends on the skill of the observer, which causes, for example, that with visibilities of 6 km, or even higher, the observer reports the appearance of haze in the present time code. Taking into account that the probability value given by the CDF considers those environments where visibility can be less than or equal to 5 km, this is an inevitable source of error, since it is very difficult to homogenize the stations information and the model forecast. Despite this, CSI values in the neighborhood of 0.5 highlight the high ability of this variable for the forecast of occurrence and temporal extent of fog/haze events. Initializations made at 0600 UTC showed lower results, justified by the inability of the model to detect the occurrence of the phenomena in the first 6 hours of run, which asserts the impact on this phenomena forecast results, of the model spin-up time.

From a general analysis for all study cases regardless of initialization time, it follows that the inner region is the one with major problems in detecting the phenomena with a marked increase in false alarms in the alpha parameter. This coincides with the findings in the analysis of absolute error, where this region had the highest values.

On the North coast, the principal problem is an increase in the number of unpredicted occurrences with respect to the other sub-regions, which caused the CSI to be lower. In this sense it should be taken into account that two of the three stations that make up the sub-region (318 and 320) lay north of the Sierra de los Órganos mountains chain. This suggest that mountain effects occur in that region, which could result in a more complex dynamical interaction of the meteorological variables and thus, under certain circumstances, it may be too demanding for the numerical model.

Overall, results obtained were more reliable towards the south coast, followed by the inner region. Note that the CDF is the variable with better results, since for the three sub-regions the probability of correct detection was above 75%, with CSI at around 0.5.

CONCLUSIONS

According to the results of this research, it is possible to confirm that the model spin-up process has influence on its ability to detect favorable environments for the genesis and evolution of fog/haze. It is also observed that the model tends to overestimate the values of the variables associated with the formation of these phenomena. The forecasted visibility values are overestimated in a range up to 10 km at the time of the phenomenon apparition, which causes that the probability of correct detection range is between 20 and 30%. Probability values obtained by the cumulative distribution function over 75% can be used in the prognosis of potentially favorable environments for fog/haze to appear. CDF was precisely the variable that best identified potentially favorable environments for genesis and evolution of fog/haze, presenting a CSI in the vicinity of 0.5 for all sub-regions. For detection of fogs/haze by numerical soundings, vertical gradients, temperature inversion and the wet layer next to surface characteristics should be considered.

REFERENCES

Alfonso A. P. & Florido A. 1993. El clima de Matanzas. Editorial Academia, La Habana, 113 pp.

Álvarez, E. L.; Borrajero, M. I.; Álvarez, M. R. & León, L. A. 2011ª. "Estudio de la marcha interanual de la frecuencia de ocurrencia de los fenómenos nieblas y neblinas a partir del código de estado de tiempo presente". *Revista Ciencias de la Tierra y el Espacio* , (12): 31-46, ISSN: 1729-3790

Bergot T.; & Guedalia D. 1994. Numerical Forecasting of Radiation Fog. Part I: Numerical Model and Sensitivity Tests. MWR, Vol. 122, No. 6, 12181230. DOI: 10.1175/1520-0493(1994)

Creighton G.; Kuchera E.; Adams-Selim R.; Mc Cormik J.; Rentschler S.; & Wickard B. 2014. AFWA Diagnostics in WRF. .

Franciscatto N.; Puhales F. S.; Anabor V.; Dal Piva, E.; de Lima, E. 2015.`` Mean weather characteristics associated to radiation fog at Santa Maria-RS``. Ciência e Natura, Santa Maria v.37 n.3, 2015, Set.- Dez. p. 613 - 624 *Revista do Centro de Ciências Naturais e Exatas - UFSMISSN* impressa: 0100-8307 ISSN on-line: 2179-460X. DOI:10.5902/2179-460X17277.

Golding B.W. 1993. ``A Study of the Influence of Terrain on Fog Development``. *Monthly Weather Review*, Vol.121, No. 9, 2529-2541.

Guzmán L. 2013. *Condiciones favorables para la ocurrencia de nieblas en Cuba.* Tesis en opción al título de Licenciado en Meteorología. Instituto Superior de Tecnologías y Ciencias Aplicadas (InsTEC), La Habana, Cuba. 85 p, Avaliable: Meteorologic Department, InsTEC, .

Hernández J. F.; González C. M.; González P. M. 2017. "Pronóstico de nieblas en las provincias de Artemisa, La Habana y Mayabeque". IX Congreso Cubano de Meteorología , La Habana, Cuba. ISBN: 978-959-7167-60-0. Avaliable: Sociedad Meteorológica de Cuba. .

Ledesma, M. & Baleriola, G. 2003. Meteorología aplicada a la aviación. 12th ed., Madrid: Thomson Paraninfo, 602 p. ISBN: 978-84-283-2840-1

Ryerson W. 2012. Toward improving short-range fog prediction in data-denied areas using the Air Force Agency Mesoscale Ensemble.

Sierra M. *et al.,* 2014. Sistema de Predicción a muy corto plazo basado en el Acoplamiento de Modelos de Alta Resolución y Asimilación de Datos. Informe de resultado. Programa: "Meteorología y Desarrollo Sostenible del País". Instituto de Meteorología. DOI: 10.13140/RG.2.1.2888.1127

Sosa M.; Rodríguez O. & Hernández R. .1992. ``Las nieblas en las Provincias Habaneras``. *Revista Cubana de Meteorología*, Vol. 5, No. 2, pp 28 34.

Lic. Pedro Manuel González Jardines. Jose Martí ,International Airport, Boyeros Ave, Havana, Cuba. E-mail: pedro.met90@gmail.com

Dra. Maibys Sierra Lorenzo. Center for Atmospheric Physics, Institute of Meteorology, Casablanca, Havana, Cuba. E-mail: maibys.lorenzo@insmet.cu

Msc. Carlos Manuel González Ramírez. Provincial Meteorological Center La Habana-Artemisa-Mayabeque. Institute of Meteorology, Casablanca, Havana, Cuba. E-mail: carlosm.gonzalez@insmet.cu

Lic. Israel Borrajero Montejo. Center for Atmospheric Physics, Institute of Meteorology, Casablanca, Havana, Cuba. E-mail: israel.borrajero@insmet.cu

Conflicts of Interest: The authors declare no conflict of interest.

Authors's contribute: Idea, data processing and paper elaboration: **Pedro M. Gonzalez Jardines**. Data processing, paper's elaboration and reviewed: **Maibys Sierra Lorenzo**. Data recopilation, synoptical analysis and paper's reviewed: **Carlos M. Gonzalez Ramirez**. Paper's elaboration and reviewed: **Israel Borrajero Montejo**.